Academic Journal of Science and Technology
ISSN: 2771-3032 | Vol. 9, No. 3, 2024

Numerical Study on the Condensation Performance of Triethylene Glycol Regenerated Exhaust Gas in Elliptical Tube

Yangjun Qiu, Liang Zhang, Jiyu Zheng, Zhongchao Yan

School of Mechanical Engineering, Southwest Petroleum University, Chengdu, Sichuan 610500, PR China

Abstract: Condensation technology has been widely applied in industries such as energy, metallurgy, refrigeration, petrochemicals, and chemical engineering. Steam condensation is a complex phase change process, and its heat transfer characteristics are significantly different from convective heat transfer without phase change. This article is based on the condensation treatment process of triethylene glycol dehydration regeneration tail gas, proposing the use of elliptical tubes instead of circular tubes for condensation of regeneration tail gas. The finite volume method was used to numerically study the condensation process of regenerated exhaust gas inside an elliptical tube, and compared with a circular tube. The effect of different structural parameters on condensation was also studied. The results show that the use of elliptical tubes can effectively improve condensation efficiency, with a maximum condensation effect of 2.04 times. The research results can provide guidance for enhancing condensation of triethylene glycol regeneration exhaust gas.

1. Introduction

The process of steam condensation is a phase change process that transforms steam into liquid and releases heat. When the saturation temperature corresponding to steam pressure is lower than the ambient temperature, the condensation phenomenon will continue to occur. The mechanism of pure steam condensation is the diffusion movement of molecules. The molecules back and forth at the interface between the steam and the liquid film diffusion. When the flow velocity of the liquid film side of the steam toward the liquid film side is higher than the velocity of the liquid film side towards the steam side, condensation occurs, and vice versa, evaporation occurs. When reaching a stable state, the flow velocities on both sides are equal. There are generally two ways of pure steam condensation: film condensation and dropwise condensation. Due to the instability of dropwise condensation, it is easy to transform into film condensation, so it is basically film condensation in industry[1-4].

The earliest theoretical study on condensation heat transfer in the world was conducted by Nusselt. Nusselt was the first to use boundary layer theory to establish equations for liquid film flow and heat transfer, and to solve for the velocity and temperature distribution of the liquid film. He obtained theoretical solutions for the condensation heat transfer coefficient and liquid film thickness of pure steam under laminar flow conditions[5]. The Nusselt classical theory has always been the theoretical basis for steam condensation research, and later the Nusselt theoretical solution was extended to vertical circular tubes[6], horizontal circular tubes[7], and spherical tubes[8].

For steam condensation processes containing non-condensable gas, they are more complex compared to pure steam condensation. For the condensation process of mixed steam containing non-condensable gas, non-condensable gas has a significant impact on the condensation process. Due to the inability of non-condensable gas to pass through the liquid film, no-condensable gas film will form during the condensation process and adhere to the tube wall. Water vapor in the mixed steam needs to pass through this non-condensable gas film to contact with the cold wall surface to condense, resulting in a significant decrease in the condensation effect. When the content of non-condensable gas is high, the non-condensable gas film will become the main thermal resistance[9-11], with a much greater impact than the liquid film thermal resistance.

A large number of domestic and foreign scholars have conducted experimental and numerical studies on the condensation process of mixed steam containing non-condensable gas. Othmer was the first to conduct experimental research on the condensation process of steam containing non- condensable gas, analyzing the effects of parameters such as steam temperature and non- condensable gas volume fraction on condensation heat transfer[12].

Hasson[13] found through experiments that a small amount of non-condensable gas can significantly reduce the condensation heat transfer coefficient of mixed steam. The experiment showed that under 1% air content, the average heat transfer coefficient decreased by about 50% -60%. Diwani and Rose's experiment also showed that under natural convection, 1% nitrogen gas can reduce the condensation rate of mixed steam by about 50%[14].

Sparrow and Minkowycz, based on the boundary layer theory, solved the boundary layer equation containing non-condensable gas[15] and found that non-condensable gas forms a diffusion boundary layer, which aggregates at the interface between the tube wall and the liquid film, reducing the condensation rate.

Li Hao studied the condensation heat transfer process inside the condenser tube in a passive safety cooling system by building a test bench. He studied two media, pure steam and a mixture containing non-condensable gas, and compared results[16]. The experimental results show that the condensation process of mixed gases significantly reduces the condensation heat transfer capacity of steam inside the tube compared to pure steam, and the heat transfer capacity decreases more with the increase of non-condensable gas content.

With the development of computer technology, more and

more scholars are studying problems through numerical simulation methods. Numerical simulation can not only solve impossible operating conditions, but also greatly save the economic and time costs of experiments.

Ge Jianying studied the condensation process of a vertical tube containing a mixture of non- condensable gas and steam using custom source term function of Fluent. He investigated the effects of factors such as pipe diameter, steam flow rate, wall temperature, wall material, and non- condensable gas content on condensation heat transfer[17]. Research has shown that the higher the steam flow velocity and the smaller the tube diameter, the lower the wall temperature, the better the heat transfer performance of low wall materials, the lower the non-condensable gas content, and the better the condensation effect of steam inside the tube.

Liu Quan used Fluent's custom function to simulate the condensation process of mixed steam containing non-condensable gas on a vertical flat plate[18]. It was found that when the content of non-condensable gas is high, the proportion of liquid film thermal resistance compared to non-condensable gas thermal resistance significantly decreases. Increasing the steam flow velocity can enhance the wall heat transfer coefficient, but the condensate flow rate decreases.

Bai Yang established a 2D model of condensation of mixed steam containing non-condensable gas on a vertical flat plate based on Fluent software. The simulation was carried out using the VOF multiphase flow model and a custom function defined condensation method, and the accuracy of the numerical simulation was verified by comparing it with experimental values[19]. The results indicate that the presence of non-condensable gas will lower the condensation heat transfer coefficient than the Nusselt theoretical value, and the thermal resistance of non-condensable gas accounts for the main position of the overall thermal resistance.

Jia Wenhua used Fluent software to numerically study the condensation of steam containing non-condensable gas in corrugated tubes, and analyzed the influence of structural parameters of corrugated tubes on condensation heat transfer efficiency[20]. Research has found that as the width of wave nodes increases and the spacing between wave nodes decreases, the heat transfer effect is better. Jia Yiqiong compared the external condensation heat transfer characteristics of circular tubes, elliptical tubes, and drop-shaped tubes through C++programming[21]. Research has found that under the same tube diameter and heat transfer area, the average heat transfer coefficient of a drop shaped cross-section tube is 1.05 times that of an elliptical tube and 1.2 times that of a circular tube.

Wang Xiaojia used Fluent software and compiled UDF based on WCM and VOF models to achieve interphase mass transfer. The condensation process on the mixed steam surface of vertical flat plates and corrugated plates was analyzed, and a new type of serrated strengthened condensation plate was proposed and compared[22]. Research has shown that serrated enhanced condensing plates have better condensing effects, can disturb steam, enhance contact between steam and plates, and weaken the influence of liquid film thermal resistance on heat transfer.

This paper is based on the condensation treatment process of triethylene glycol dehydration regeneration exhaust gas, proposing the use of elliptical tube instead of circular tube for condensation of regeneration exhaust gas. A numerical study was conducted on the condensation process of regenerated exhaust gas inside elliptical tube using the finite volume method, and compared with the circular tube. The effect of steam flow velocity, wall temperature, non-condensable gas content, and structural parameters on the condensation effect were discussed

2. Numerical Model

2.1. Physical model

This study works on the condensation process of water vapor containing non-condensable gas inside an elliptical tube. The non-condensable gas is air, and the fluid domain model of the elliptical tube is shown in Fig.1. The long axis $a = 20.4$ mm, the short axis b =10.2 mm, and the tube length L =1000 mm. Table 1 shows actual dimensions of elliptical tube with different long short ratio under the same equivalent diameter. Table 2 shows main content of different chapters.

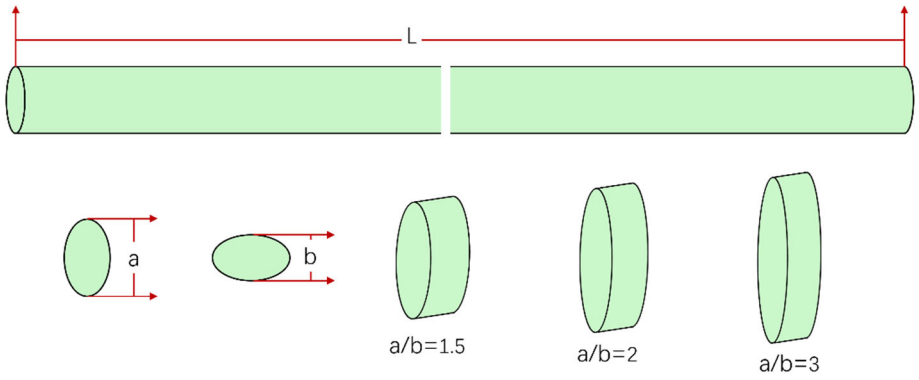

Figure 1. Detailed view of the test section

Table 1. Actual dimensions of elliptical tube with different long short ratio under the same equivalent diameter

a/mm	b/mm	a/b	L/mm
16.5	11	1.5	1000
20.4	10.2	2	1000
28.5	9.5	3	1000

Table 2. Structure parameters of different chapter

Chapter	Velocity	a/b	Wall Temperature Tw (K)	Volume fraction of non-condensable gas	Note
3.2	1	2	293	0.1	Mechanism study
3.3	1, 2, 3, 4, 5	2	293	0.1	Velocity study
3.4	1	1.5, 2, 3	293	0.1	a/b study
3.5	1	2	273K, 293K, 303K	0.1	Wall temperature study
3.6	1	2	293K	0.01, 0.04, 0.07,0.1	Non-condensable study

2.2. Governing equations and condensation numerical model

This article uses single-phase multi-component transport equations to describe the flow and heat transfer characteristics of water vapor containing non-condensable gas in an elliptical tube channel. The basic control equations used for calculation are shown below.

Continuity equation:

$$\frac{\partial \rho}{\partial t} + \nabla(\rho \vec{u}) = S_m \tag{1}$$

momentum equation:

$$\frac{\partial(\rho \vec{u})}{\partial t} + \nabla(\rho \vec{u}\vec{u}) = -\nabla p + \rho f + S_{mon} \tag{2}$$

Energy equation:

$$\frac{\partial(\rho E)}{\partial t} + \nabla(\rho \vec{u} E) = \rho f \vec{u} + \nabla(\rho \vec{u}) + \nabla(k_{eff} \nabla T) + S_h \tag{3}$$

Composition equation:

$$\frac{\partial(\rho \omega_j)}{\partial t} + \nabla(\rho \vec{u} \omega_j) = \nabla(\rho D_j \nabla \omega_j) + S_j \tag{4}$$

Among them: ρ is for density; $\vec{u}$ is velocity, S_m is the quality source term; p is surface force; f is the volumetric force; S_{mon} is the momentum source term; E is energy; k_{eff} is thermal conductivity coefficient; S_h is the energy source term; ω is the mass fraction, D is the diffusion coefficient, and the subscript j represents the gas component.

Numerical simulation is based on diffusion theory and defines the mass transfer process by adding source terms to the control equation. During the simulation process, the following assumptions are followed:

(1) The non-condensable gas film is the main thermal resistance in the condensation heat transfer process, so the liquid film thermal resistance is ignored, and it is considered that the temperature of the gas-liquid interface is the same as the temperature of the condensation wall.

(2) This article mainly studies the heat transfer performance of the condensation interface under different operating parameters, and the shape and thickness of the liquid film change relatively little after full development. Therefore, it is assumed that the liquid film does not change with the variation of various parameters.

(3) The mixture of steam and air is assumed to be an ideal gas, without considering the effect of wall radiation on steam condensation.

(4) The condition for condensation to occur is that the vapor partial pressure near the wall is greater than the saturation pressure corresponding to the wall temperature. Condensation occurs at the first layer of grid near the condensation wall, and the vapor saturation pressure is related to temperature. It is determined by the following formula:

$$P_{sat} = \exp\left[\frac{c_1}{T} + c_2 + c_3 T + c_4 T^2 + c_5 T^3 + c_6 T^4 + c_7 \ln(T)\right] \tag{5}$$

Among them: c_1=-5800.2206，c_2=1.3914993，c_3=-0.04860239，c_4=4.1764768e-05，c_5=1.4452093e-08，c_6=0，c_7=6.54259673。

The mass source term added to the continuity equation can be defined as follows:

$$S_m = \frac{\omega_v}{\omega_v - 1} \rho D \frac{\partial \omega_v}{\partial n} \frac{A_{cell-wall}}{V_{cell}} \tag{6}$$

In the formula, ω_v is the mass fraction of water vapor, $\frac{\partial \omega_v}{\partial n}$ is the gradient of steam mass fraction at the gas-liquid interface, $A_{cell\text{-}wall}$ wall is the area of the condensing wall unit, V_{cell} is the volume of the near wall unit, D is the diffusion coefficient, defined according to the following equation:

$$D = D_0 (\frac{P}{P_0})^{-1} (\frac{T}{T_0})^n, n=1.81 \tag{7}$$

The flow process of steam from adjacent units on the wall will cause power loss, which can be represented by the following momentum source term:

$$S_{mon} = S_m U_n \tag{8}$$

Among them, U_n is the gas flow velocity along the n-direction.

The energy source term is represented as the product of the mass source term and latent heat, as shown below:

$$S_h = S_m h \tag{9}$$

To evaluate the flow and heat transfer characteristics of water vapor containing non-condensable gas in an elliptical tube, the following dimensionless numbers are defined:

Condensation heat transfer coefficient:

$$h = \frac{\Phi}{A_t (T_{wall} - T_m)} \tag{10}$$

resistance coefficient:

$$f = \frac{2\Delta p D_e}{\rho u_i^2 L} \tag{11}$$

Nusselt number:

$$Nu = \frac{hL}{\lambda_l} \tag{12}$$

Comprehensive heat transfer index:

$$PEC = \frac{Nu / Nu_0}{(f / f_0)^{1/3}} \tag{13}$$

Among them, Φ It is the heat transfer rate, A_t is the tube wall area, T_{wall} and T_m are the wall temperature and the average temperature of the calculation domain, Δp is the pressure drop, D_e is the equivalent diameter, and L is the tube length, λ_l is the thermal conductivity coefficient, u_i is the average velocity of the fluid, Nu_0, f_0 is the value of the circular tube under the same conditions.

2.3. Boundary conditions and simulation settings

The boundary conditions used in the simulation are: the inlet is set as the velocity inlet, and velocity range of the water vapor containing non-condensable gas at the inlet is $1\sim5m/s$. Under initial conditions, the non-condensable gas is set as air and the air mass fraction is 0.1. and the temperature of the water vapor containing non-condensable gas at the inlet is $373K$, with condensing wall temperature of $293K$. The numerical simulation uses an implicit coupled solver to perform transient solutions on a three-dimensional mesh, with a time step of 2×10^{-5} s and 50 iterations per step. Numerical simulation adopts k-ε turbulence model, The turbulence model has better adaptability to boundary layer, separation, and recirculation flow under rotation, strong reverse pressure gradient. The $PISO$ algorithm is used to couple the pressure and velocity, and the pressure correction term is discretized in a second-order upwind format. The momentum, turbulence energy, dissipation rate, composition, and energy equations are discretized in a second-order upwind format.

3. Results and Discussion

3.1. Model validation

Based on the experimental conditions in reference[23], a numerical model was established using the numerical method in this paper to compare the simulation results with experimental data. The experimental conditions are shown in Figures 2 and 3. The experimental object is a horizontal tube with a length of 3.37 meters and a diameter of R=0.0475 meters. The lengths of the insulation section and the condensation section are 0.81 m and 2.4 m, respectively. Simplify the computational domain into an axisymmetric two-dimensional model, and set the condensation wall temperature to vary with a polynomial function, shown in Fig.2. The mass flow rate at the inlet is 0.01667kg/s, the temperature is 418.45K, and the mole fraction of air is 0.148. The temperature and wall heat flux on the centerline were calculated, as shown in Fig.3. The relative error in temperature observed on the centerline is less than 1%. In addition, the relative error of wall heat flux is less than 15%. Therefore, the numerical model presented in this article can be considered a reasonable computational method.

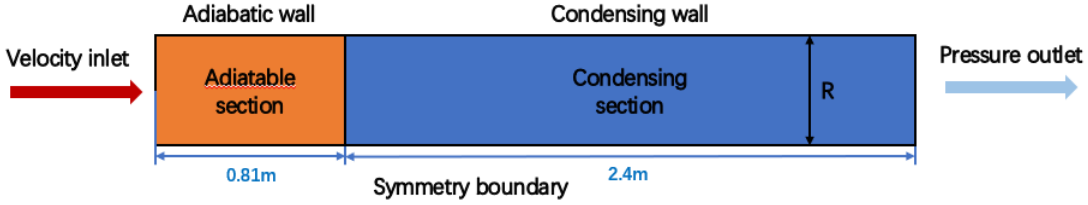

Figure 2. Detailed view of validation model

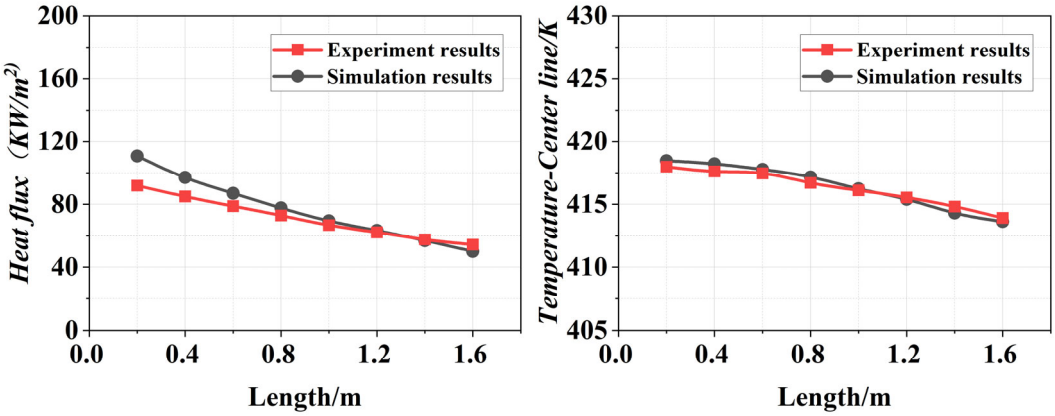

Figure 3. Validation of numerical model

3.2. Flow and condensation heat transfer characteristics

The condensation heat transfer inside the elliptical was numerically simulated under the conditions of a mixed steam velocity of 1m/s, a non-condensable gas content of 10%, a/b ratio of 2 of the elliptical tube, and a wall temperature of 293K.

The Fig.4 shows the temperature distribution contour of the fluid inside the elliptical tube It can be seen from the figure that the temperature in the middle mainstream area of the tube is higher, the wall temperature is lower, and the fluid temperature gradient is larger in the near wall area; The fluid inside the pipe gradually cooled, and the low temperature zone near the wall gradually increases. The Fig.5 depicts the temperature distribution of different cross-sections along the flow direction. It can be seen from the figure that the average temperature of the cross-section gradually decreases along the flow direction.

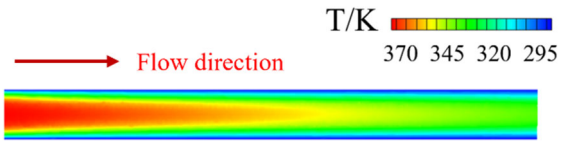

Figure 4. Temperature distribution along the flow direction

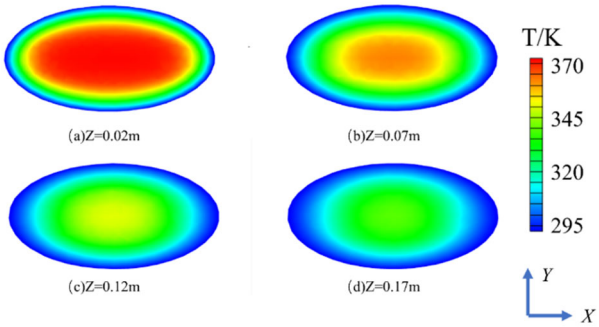

Figure 5. Temperature distribution of different cross-sections along the flow direction

The Fig.6 shows the distribution contour of fluid velocity inside the pipe. It can be seen from the figure that the velocity in the central mainstream area of the tube is higher, while the velocity in the near wall area is lower. Along the flow direction, the high-speed area in the mainstream area gradually becomes smaller. The Fig.7 depicts the flow velocity distribution along different cross-sections along the flow direction. It can be seen that the average velocity of the cross-section decreases along the flow direction, and the velocity decreases faster at the left and right ends of the elliptical tube. This is because fluid erosion and impact on the pipe wall generate kinetic energy loss, as well as the liquid film generated by condensation adhering to the pipe wall, creating viscous shear resistance on the fluid.

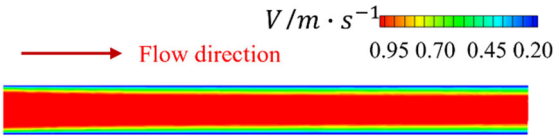

Figure 6. Velocity distribution along the flow direction

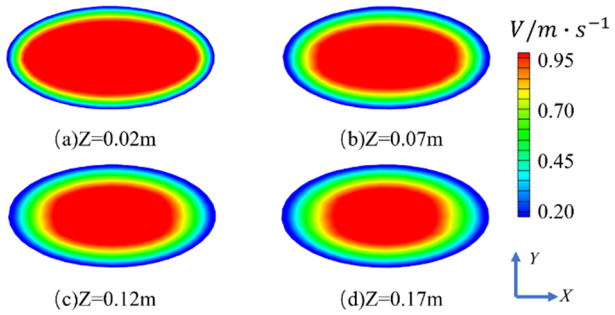

Figure 7. Velocity distribution of different cross-sections along the flow direction

The Fig.8 shows the distribution of air volume fraction at different cross-sections along the flow direction. From the Fig.8, it can be seen that the air forms a diffusion layer gas film near the condensation wall, and the thickness of the air film gradually increases along the flow direction. The Fig.9 depicts the distribution of water vapor volume fraction at different cross-sections along the flow direction. From the Fig.9, it can be seen that the volume distribution of water vapor is opposite to that of air. The volume fraction of water vapor near the wall gradually decreases along the flow direction. This is because air forms a diffusion layer gas film on the wall, which hinders the contact of water vapor with the wall.

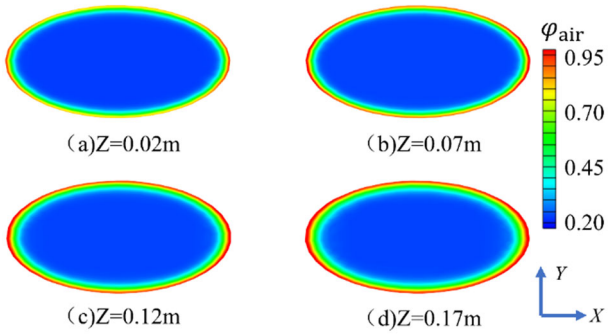

Figure 8. Air volume fraction of different cross-sections along the flow direction

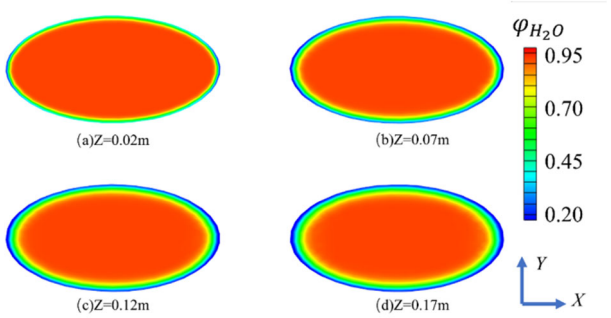

Figure 9. Water vapor volume fraction of different cross-sections along the flow direction

The Fig.10 describes the variation curves of Nusselt number Nu and resistance coefficient f for elliptical and circular pipes under different flow velocities. Fig.10 shows that as the velocity increases, Nu of the circular tube shows an approximately linear upward trend, and Nu of circular increases by 75.2% at velocity of 1m/s compared to that at 5m/s. The Nusselt number of the elliptical tube decreases

within velocity range of 1m/s to 2m/s, and shows a linear upward trend within the range of 2m/s to 5m/s. The flow resistance f of circular and elliptical tubes decreases with the increase of flow velocity, but the downward trend gradually slows down. The Nu and f of the elliptical tube are always greater than those of the circular tube. The Nu of the elliptical tube increased by about 50.7%~204.7% compared to the circular tube, and the flow resistance f increased by about 217.6%~343.8%. This is because relative friction occurs between the fluid flow and the wall, hindering the fluid movement. The velocity of the fluid near the wall significantly decreases, and the fluid near the wall almost stops, and a thin flow boundary layer is formed near the wall which hinders heat transfer. As the velocity increases, the gas-liquid shear force at the gas-liquid interface increases, and the fluid has a stronger scouring effect on the wall. The flow boundary layer becomes thinner, and the thermal resistance of condensation decreases. At the same time, the Nu increases.

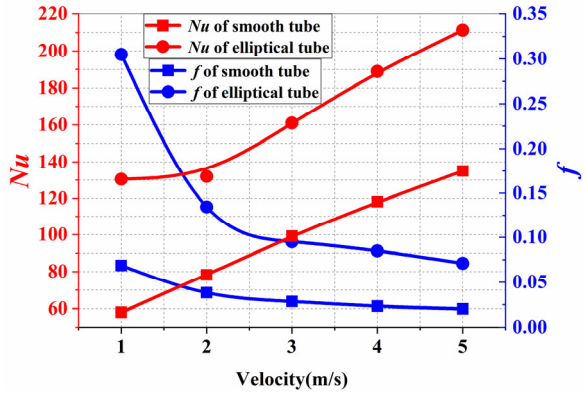

Figure 10. Comparison of Nu and f for elliptical tube and smooth tube

3.3. The effect of velocity on condensation heat transfer in elliptical tube

The Fig.11 shows the average temperature distribution of the fluid along the flow direction of the elliptical tube under the same wall temperature and air content, and different steam flow velocities. It can be seen from the Fig.11 that the average temperature of the fluid shows the same distribution trend at different flow velocities. As the flow velocity increases, the average temperature of the fluid increases, and the increasing trend gradually slows down. The flow velocity increases from 1m/s to 5m/s, and the average temperature of the fluid increases by about 6.1%. Because as the steam flow velocity increases, the fluid residence time of fluid in the tube becomes shorter. Within the scope of investigation, when the flow velocity is within the range of 1m/s~2m/s, increasing the flow velocity results in a more significant decrease in the average fluid temperature. When the flow velocity is greater than 2m/s, the decrease in the average fluid temperature slows down as the flow rate increases.

As shown in the Fig.12, with the increase of flow velocity, the Nu/Nu_0, f/f_0,and PEC of the elliptical tube all show a decreasing trend. When the flow velocity is greater than 2m/s, the decreasing trend becomes slower. Therefore, when the steam flow velocity is relatively low, elliptical tubes have a significant improvement in heat transfer efficiency compared to circular tubes.

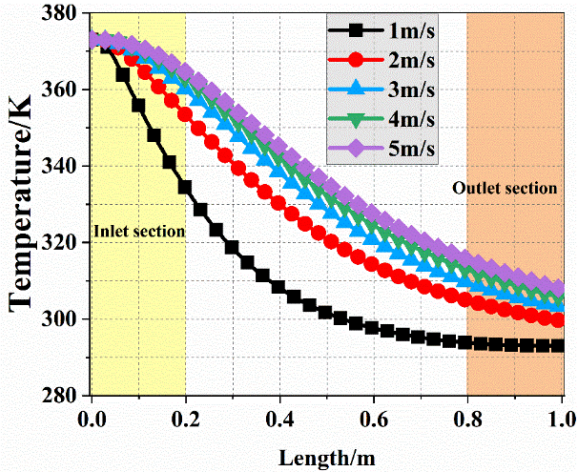

Figure 11. Average temperature distribution along the flow direction

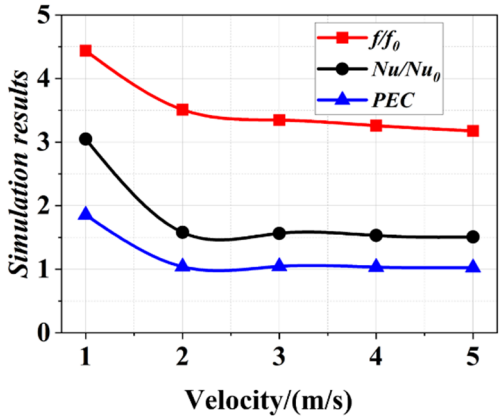

Figure 12. Simulation results of Nu/Nu_0, f/f_0,and PEC with different velocities

3.4. The effect of long short axis ratio on condensation heat transfer

The Fig.13 shows the distribution of average fluid temperature along the flow direction for the elliptical tube with different long and short axis ratios, under the same wall temperature and air content, and at the same steam flow rate. It can be seen from the Fig.13 that the average fluid temperature shows the same distribution trend under different long and short axis ratios. As the long and short axis ratio increases, the decrease in average fluid temperature is very small. Fig.14 shows that as the long short axis ratio increases, the Nusselt number Nu decreases. The long short axis ratio increases from 1.5 to 3, and Nu decreases by about 0.5% to 17.7%. Within the research scope, as the flow velocity increases, the Nu of elliptical tubes under different long short axis ratios shows the same trend of change: decreasing in the range of flow velocity of 1m/s~2m/s and linearly increasing in the range of 2m/s~5m/s. Moreover, as the long short axis ratio increases, the Nu of elliptical tube decreases faster.

The effect of different long short axis ratios on the Nu/Nu_0, f/f_0, and PEC of elliptical tubes is shown in the Fig.14. As the long short axis ratio of elliptical tubes increases, both Nu/Nu_0 and $PEC$of elliptical tubes decrease, while the increase in long short axis ratio has little effect on f/f_0. As the flow velocity increases, the Nu/Nu_0, f/f_0 and PEC of the elliptical tube all show a decreasing trend. Therefore, with a relatively small long short axis ratio, elliptical tubes have a more significant improvement in heat transfer efficiency

compared to circular tubes.

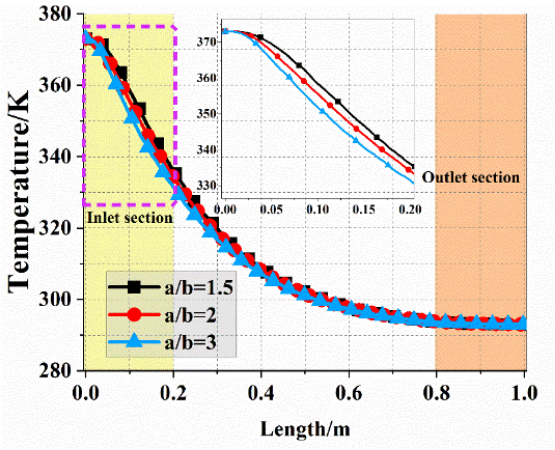

Figure 13. Comparison of average temperature distribution along the flow direction for elliptical tubes with different long short axis ratio

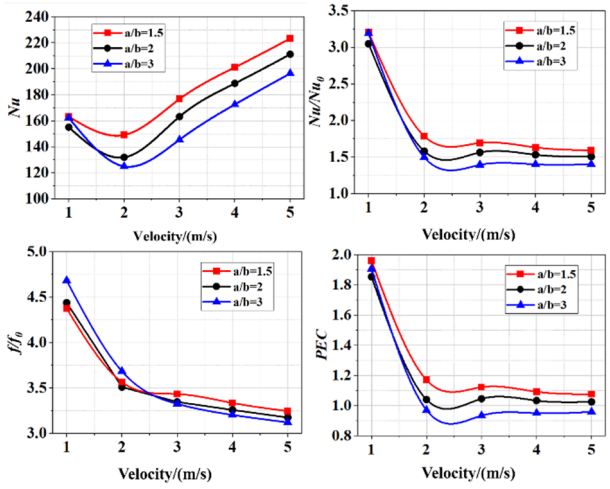

Figure 14. The effect of long short axis ratio on condensation heat transfer

3.5. The effect of wall temperature on condensation heat transfer

The Fig.15 shows the average temperature distribution of the fluid along the flow direction for the elliptical tube with different wall temperatures, under the same steam flow rate and air content. The Fig.15 shows that the average temperature of the fluid shows the same distribution trend at different wall temperatures. As the wall temperature increases, the average temperature of the fluid increases. The wall temperature increases from 273K to 303K, and the average fluid temperature increased by 9.7%. The Fig.16 shows the distribution of Nusselt number Nu under different wall temperatures. It can be seen that as the wall temperature increases, the Nusselt number increases. The wall temperature increases from 273K to 303K, and *Nu* increases by about 12.5% to 16.8%. This is mainly due to the increase in wall temperature, which reduces the driving force of condensation. When the latent heat of vaporization remains constant, the total heat transfer also decreases, the condensation resistance decreases, and the Nusselt number increases. Within the scope of the study, as the flow velocity increases, the *Nu* of elliptical tube shows the same trend at different wall temperature: decreasing in the range of flow velocity of 1m/s~2m/s and linearly increasing in the range of 2m/s~5m/s.

The effects of different wall temperatures on the Nu/Nu_0, f/f_0, and PEC of circular tubes are shown in the Fig.15. As the wall temperature of the elliptical tube increases, the f/f_0 of the elliptical tube decreases. The increase in wall temperature has almost little effect on Nu/Nu_0 and PEC. As the flow velocity increases, the Nu/Nu_0, f/f_0 and PEC of the elliptical tube all show a decreasing trend.

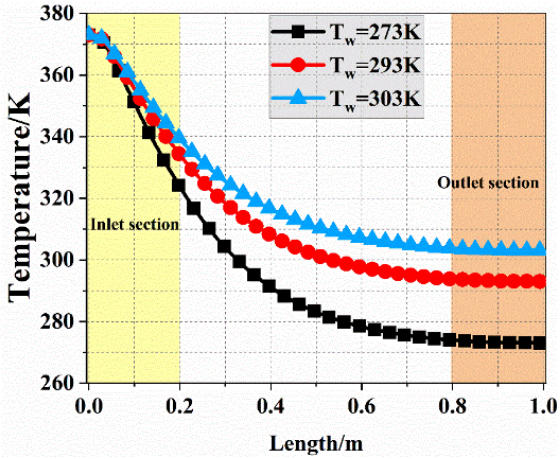

Figure 15. Comparison of average temperature distribution along the flow direction for elliptical tubes with different wall temperature

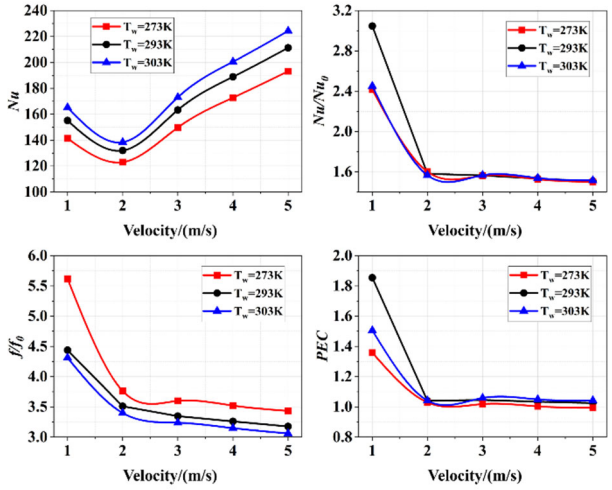

Figure 16. The effect of wall temperature on condensation heat transfer

3.6. The effect of non-condensable gas content on condensation heat transfer

The Fig.17 shows the average fluid temperature distribution along the flow direction of the elliptical tube under the same wall temperature and steam flow rate, but with different non-condensable gas content. It can be seen from the Fig.17 that the average fluid temperature has the same distribution trend under different non-condensable gas contents. With the increase of non-condensable gas content, the average fluid temperature increases, but the increase is not significant. The Fig.18 shows the distribution of Nusselt number under different non-condensable gas contents. It can be seen from the Fig.18 that as the non-condensable gas content of the fluid increases, the Nusselt number Nu of the elliptical tube decreases, and the magnitude of the reduction

decreases with the increase of non-condensable gas content. The non-condensable gas content increases from 0.01 to 0.1, and *Nu* increases by about 31.9% to 49%. Within the research scope, as the flow velocity increases, the Nusselt number of the elliptical tube shows the same trend under different non-condensable gas contents.

The effect of different non-condensable gas content on the Nu/Nu_0, f/f_0 and PEC of the elliptical tube are shown in the Fig.18. As the non-condensable gas content increases, the Nu/Nu_0, f/f_0 of the elliptical tube all decrease. When the non-condensable gas content is 0.07, the elliptical tube has the maximum Nu/Nu_0, f/f_0 of the elliptical tube all decrease. The PEC of the elliptical tube with non-condensable gas content of 0.1 first decreases and then increases.

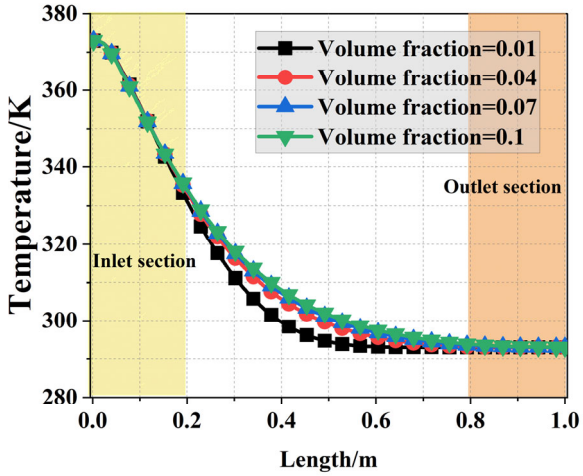

Figure 17. Comparison of average temperature distribution along the flow direction for elliptical tubes with different non-condensable gas content

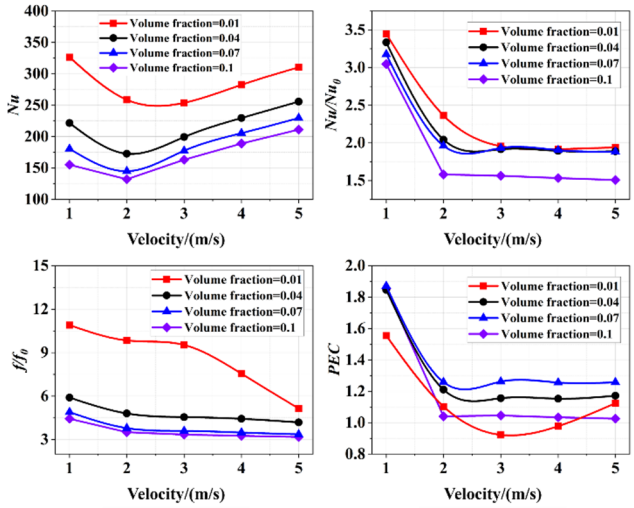

Figure 18. The effect of non-condensable gas content on condensation heat transfer

4. Conclusion

This paper is based on the condensation treatment process of triethylene glycol dehydration regeneration exhaust gas, proposing the use of elliptical tube instead of circular tube for condensation of regeneration exhaust gas. A numerical study was conducted on the condensation process of regenerated exhaust gas inside elliptical tube using the finite volume method, and compared with the circular tube. The effect of steam flow velocity, wall temperature, non-condensable gas content, and structural parameters on the condensation effect were discussed, and the main conclusions were drawn as follows:

1. The velocity and temperature distribution of steam inside an elliptical tube exhibit an elliptical shape. Along the flow direction, the thickness of the air diffusion film on the condensing wall increases, hindering the condensation of water vapor, resulting in a gradual decrease in the volume fraction of water vapor near the wall along the flow direction.

2. The Nu and f of the elliptical tube are always greater than those of the circular tube. The Nusselt number of the elliptical tube is increased by about 50.7%~204.7% compared to the circular tube, and the flow resistance f is increased by about 217.6%~343.8%.

3. The steam flow velocity, non-condensable gas content, and tube wall temperature all affect the condensation heat transfer efficiency inside the elliptical tube. Within the scope of investigation, the higher the steam flow velocity, the lower the content of non-condensable gas, the greater temperature difference between the tube wall and steam, the larger the Nusselt number on the tube wall, and the better the condensation heat transfer effect inside the tube.

Declaration of Competing Interest

The authors declare that they have no known competing financial interests or personal relationships that could have appeared to influence the work reported in this paper.

CreditT authorship contribution statement

Yangjun Qiu: Methodology, Software, Writing – original draft, Software. Liang Zhang: Data curation, Conceptualization. Jiyu Zheng: Visualization, Investigation. Zhongchao Yan: Supervision, Validation.

References

[1] Zhang, X., Z. Ren and F. Mei, Heat Transfer. 1993: Beijing: China Construction Industry Press. 303.

[2] Goldstein, R.J.R.M., et al., Heat transfer—A review of 2005 literature. International Journal of Heat and Mass Transfer, 2010(No.21-22): p. 4397-4447.

[3] Goldstein, R.J.R.M., et al., Heat transfer—a review of 2002 literature. International Journal of Heat and Mass Transfer, 2005(NO.5): p. 819-927.

[4] Goldstein, R.J.R.M., et al., Heat transfer – a review of 2000 literature. International Journal of Heat and Mass Transfer, 2002(NO.14): p. 2853-2957.

[5] Nusselt, The condensation of water vapor on surfaces [J]. Zeitschrift Vereines Deutscher Ingenieure, 1916. 541-546(60-9).

[6] Nusselt, Heat exchanger in the falling film condensation of water vapour on cooler [J]. Zeitsehrift Vereines Deutscher Ingenieure, 1923(67-17): p. 201-206.

[7] Dhir, V. and J. Lienhard, Laminar Film Condensation on Plane and Axisymmetric Bodies in Nonuniform Gravity. Journal of Heat Transfer, 1971(No.1): p. 97-100.

[8] Boguslawski, C.O.P.L., Heat transfer by laminar film condensation on sphere surfaces. International Journal of Heat and Mass Transfer, 1975(NO.12): p. 1486-1488.

[9] Kuhn, S.Z., V.E. Schrock and P.F. Peterson, An investigation of condensation from steam-gas mixtures flowing downward inside a vertical tube. Nuclear Engineering and Design, 1997(No.1): p. 53-69.

[10] Chen, C.O. and Y. Lin, Laminar film condensation from a downward-flowing steam-air mixture onto a horizontal circular

tube. Applied Mathematical Modelling, 2009(No.4): p. 1944-1956.

[11] Kim, M.H. and M.L. Corradini, Modeling of condensation heat transfer in a reactor containment. Nuclear Engineering and Design, 1990(NO.2): p. 193-212.

[12] DF, O., The condensation of steam [J]. Industrial and Engineering Chemistry, 1929. 21(6): p. 576-583.

[13] Hasson D, L.D.N.U., An experimental study of steam condensation on a laminar water sheet [J]. International Journal of Heat and Mass Transfer, 1964. 7(9): p. 983-1001.

[14] H. K AI Diwani, J.W.R., Free convection film condensation of steam in the presence of noncondensable gases. Heat Mass Transfer, (16): p. 1359-1369.

[15] Sparrow, E.M., W.J. Minkowycz and M. Saddy, Forced convection condensation in the presence of noncondensables and interfacial resistance. International Journal of Heat and Mass Transfer., 1967(No.12): p. 1829-1845.

[16] Hao, L., Research on condensation heat transfer characteristics of air steam mixture gas in a horizontal tube. 2016, Harbin Engineering University.

[17] Jianying, G., Numerical simulation of condensation heat transfer of steam and steam containing non-condensable gas in vertical and inclined tubes. 2020, Inner Mongolia University of Science and Technology.

[18] Quan, L., Numerical study on condensation of pure steam and steam containing non-condensable gas. 2015, University of Science and Technology of China.

[19] Yang, B., Numerical simulation and visualization experimental research on condensation heat transfer of nitrogen vapor containing non-condensable gas. 2017, Zhejiang University.

[20] Wenhua, J., Numerical simulation of condensation heat transfer characteristics of mixed gas flow in irregular tubes. 2019, Shandong University.

[21] Yiqiong, J., Research on the condensation heat transfer characteristics of non-condensable gas outside a horizontal single tube. 2018, North China Electric Power University (Baoding).

[22] Xiaojia, W., Numerical simulation of condensation heat transfer characteristics of steam containing non condensable gas on different vertical irregular surfaces. 2020, Shandong University.

[23] Kuhn, S.Z., V.E. Schrock and P.F. Peterson, An investigation of condensation from steam-gas mixtures flowing downward inside a vertical tube. Nuclear Engineering and Design, 1997(No.1): p. 53-69.